

# PREDICTION METHOD OF OPENING JET PLUME BEHAVIOUR IN THE PRESENCE OF AN OPENING SOFFIT

Y. Ohmiya<sup>a</sup>, S. Yusa<sup>a</sup>, K. Matsuyama<sup>b</sup> and K. Harada<sup>c</sup>

a. Building Research Institute, Independent Administrative Institution

b. Tokyo University of Science

c. Kyoto University

JAPAN

## ABSTRACT

When a fire breaks out and spreads in a building, high-temperature jet plumes ejected from windows can cause fire to spread to adjoining floors or neighboring buildings. Studies on jet plumes spouting from openings have previously been carried out, including the well-known pioneering work of Yokoi who presented theoretical and experimental findings on the temperature distributions and other properties of jet plumes<sup>1-4</sup>. His study, however, did not thoroughly cover situations where soffits were placed around openings from which plumes were ejected. His investigation covered situations where a soffit was placed at the upper end of an opening, but did not cover situations where a soffit was placed vertically distant from the upper end of an opening. More detailed studies on the effects of soffits are required in consideration of recent designs because there are various combinations of opening conditions, such as opening height and width, and soffit conditions, such as soffit length, in existing buildings. Against this backdrop, the present study aims to investigate systematically the behaviour of jet plumes by carrying out a compartment model experiment with various soffit lengths and various distances between the soffit and the upper end of the opening.

## EXPERIMENTAL OUTLINE

The behaviour of a jet plume ejected from an opening of a room on fire was investigated in a compartment model experiment. To verify the applicability of compartment model results to full-scale

situations, two geometrically similar scale models were studied to see whether they result in similar jet plume behaviours.

### Experimental equipment

Two types of compartment models made of perlite boards were prepared: a small-size model of 0.5 m wide, 0.5 m deep, and 0.5 m high; and a medium-size model of 1.5 m wide, 1.5 m deep, and 1.5 m high. A 20 mm thick perlite board was used as a soffit in either model. There was an opening and no forced ventilation in the compartment.

A gas burner was used as the source of fire, and the source plane was set to the floor level at the center of the compartment model. The source plane had dimensions of 0.1 m x 0.1 m in the small-size model and 0.3 m x 0.3 m in the medium-size model. The supply rate of fuel (methane gas) to the burner was controlled by using a Stech's mass flow controller.

To investigate jet plume behaviours, temperature distribution was measured as shown in Figure 1 by using type-K thermocouples of 0.32 mm in diameter. Within each compartment model, a vertical array of ten thermocouples (located at intervals 'd' of 0.05 and 0.15 m in the small- and medium-size models, respectively) were installed at each of two locations: the near right corner and the far left corner from the opening. Thermocouples were also installed between the upper and lower ends of the opening at points that divide the opening height into nine equal parts to measure the vertical distribution of jet plume temperatures<sup>5</sup>. Temperatures of a jet plume projecting from the opening were measured with thermocouples arranged as shown in Figure 1 to form a grid with spacings 'd', while one of the rows stemmed from the center of the opening. Temperatures at the far end of the soffit were measured by thermocouples arranged at intervals of 0.4d along the end.

### Experimental conditions

The heat release rates shown in Table 1 were used for different opening sizes, and soffit lengths and levels were varied as shown in Table 2. Here, soffit length  $L_s$  and soffit height  $H_s$  are defined as shown in Figure 1. The soffit widths (0.6 m and 1.8 m in the small- and medium-size models, respectively) were selected to be longer than the compartment widths.

**Table 1:** Opening conditions and heat release rates.

Aspect ratio (2B/H)	Small-size model			Medium-size model		
	B	H	HRR(kW)	B	H	HRR(kW)
4	0.2	0.1	1.8	0.6	0.3	28.7
2	0.2	0.2	5.2	0.6	0.6	81.3
1	0.1	0.2	2.6	0.3	0.6	40.6

B: Opening width(m), H: Opening height(m)

**Table 2:** Length and height of opening soffit.

Opening soffit	Length Ls(m)	Small-size	0.1	0.15	0.2	0.25	0.3	0.4
		Medium-size	0.3		0.6		0.9	1.2
	Heigh Hs(m)	Small-size	0	0.1	0.2	0.3	0.4	
		Medium-size	0	0.3	0.6			

### Experimental method

Measurements were started after the gas burner was ignited and temperatures in the compartment became nearly constant. Each set of measurements lasted for 30 s at 2 s intervals, and the average temperature during each 30 s period was used for later analysis.

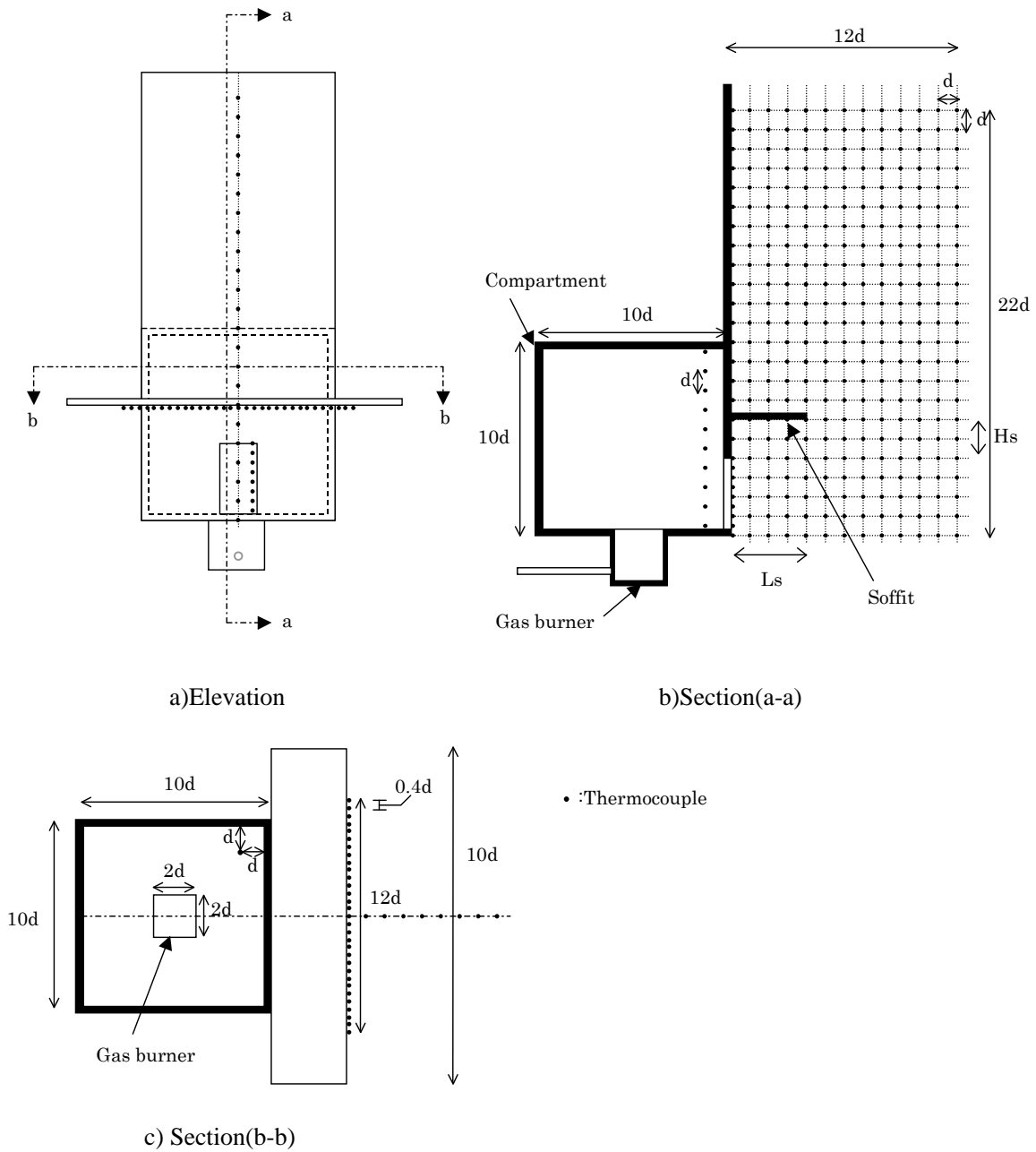


**Figure 1:** Schematic diagram of experimental apparatus.

## RESULTS AND DISCUSSION

### Vertical distribution of jet plume temperatures at the opening

Yokoi found that the position of a jet plume axis and the distribution of plume temperatures depend on the aspect ratio of the opening ( $n=2B/H$ , where B is opening width and H is opening height). This is because the jet plume ejects mostly from the upper part of the opening if temperature is assumed to be uniform in the compartment on fire. Accordingly, the vertical distribution of plume temperatures at the opening is related to the behaviour of the ejected plume. The width of the jet plume was calculated from the temperature distribution measured by the thermocouples installed at the opening. The N% method proposed by Cooper et al<sup>6</sup>. was used for this calculation, while an N-value of 10 was selected based on the measured distribution.

The cross sectional dimensions of jet plumes deduced by the above method for different opening sizes are summarised in Table 3. While the values in Table 3 represent situations without a soffit, nearly equal values were obtained for situations with a soffit.

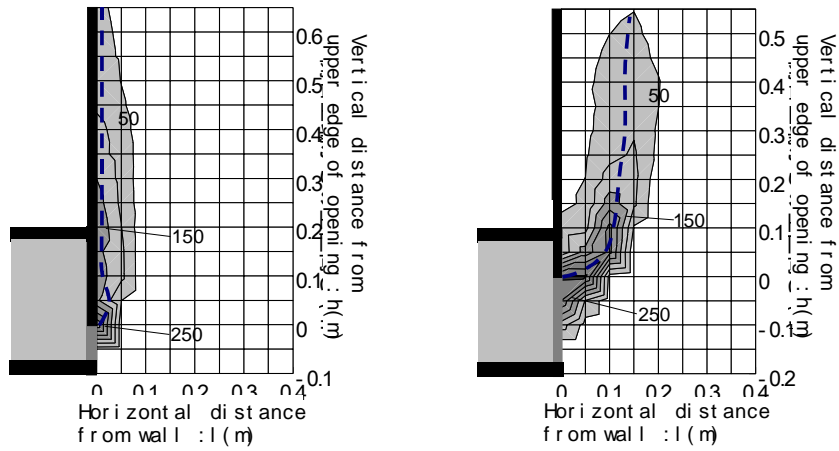
**Table 3:** Cross sectional dimensions of jet plumes.

	B	H	Thickness of External Flame(m)
Small-size	0.1	0.2	0.085
	0.2	0.2	0.074
	0.2	0.1	0.035
Medium-size	0.3	0.6	0.27
	0.6	0.6	0.25
	0.6	0.3	0.1

B: Opening width (m), H: Opening height (m)

### Temperature distribution of an ejected plume

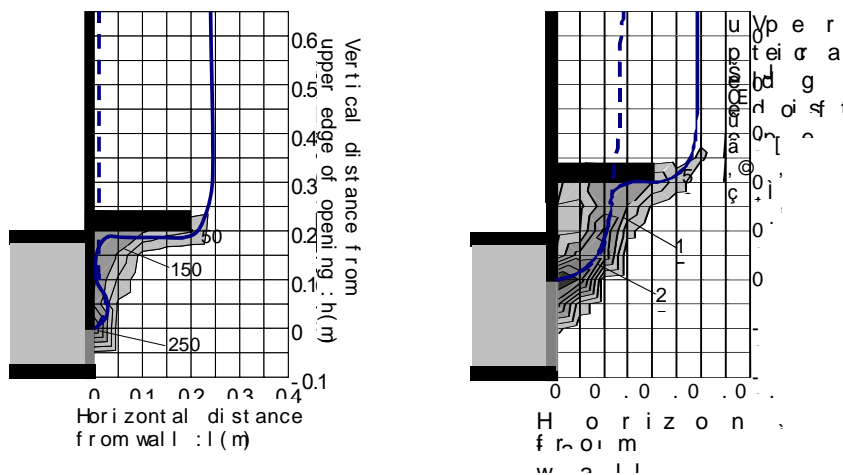
The measured distributions of jet plume temperatures are shown in Figure 2 for situations without a soffit and with a soffit (length and height are both 0.2 m). The opening size (width x height) was either 0.2 m x 0.1 m or 0.1 m x 0.2 m. The figure indicates that the position of the plume axis below the soffit is almost unchanged regardless of the presence of the soffit. When the plume hits the soffit, the region of high temperatures extends laterally along the soffit. The presence of the soffit causes higher temperatures in the region between the opening and the far end of the soffit. When there is no soffit, the distribution of high temperatures extends upward to higher levels.



1. 0.2 m(B) x 0.1 m(H)

2. 0.1 m(B) x 0.2 m(H)

a) Situation without soffit.



1. 0.2 m(B) x 0.1 m(H)

2. 0.1 m(B) x 0.2 m(H)

b) Situation with soffit.

**Figure 2:** Temperature distribution of a jet plume from opening (Soffit height and length are both 0.2 m: Temperature interval is 50 degrees).

### Temperature distribution along the soffit

Figure 3 shows, for each opening size, the temperature distribution at the level of 5 mm below the soffit of the soffit placed at a height of 0.2 m in the small-size model. The horizontal and vertical axes represent distance from the wall and temperature rise, respectively, and the curves correspond to different soffit

lengths. The results indicate that temperature distribution along the soffit does not vary widely with soffit length for the same opening size. However, markedly low temperatures were observed for a soffit length of 0.1 m and opening sizes (width x height) of 0.2 m x 0.2 m and 0.1 m x 0.2 m; this suggests that the plume axis did not hit the soffit in these cases.

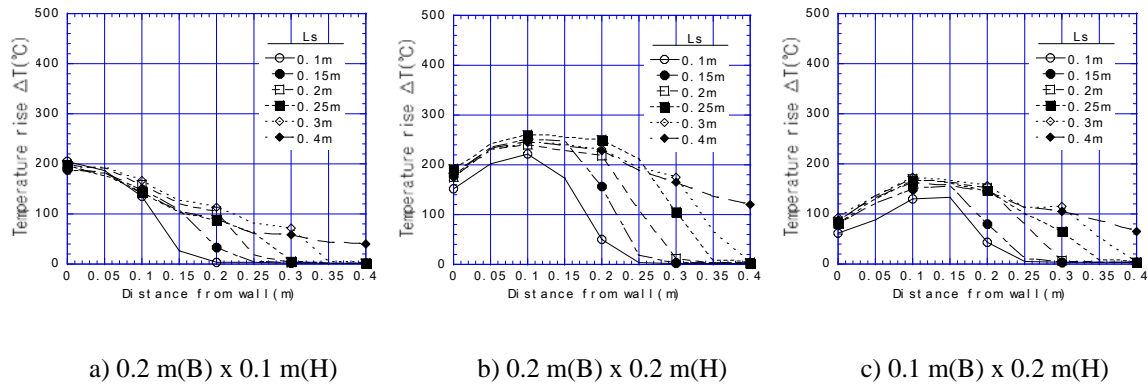


**Figure 3:** Temperature distribution beneath the soffit placed at a height of 0.2 m in the small-size model.

Figure 4 shows, for each opening size, temperature distribution beneath the soffit of the soffit (0.4 m long) placed at different heights in the small-size model. Temperatures beneath the soffit tend to decrease as the soffit level is raised. In the case of an opening width of 0.2 m and an opening height of 0.1 m, the maximum temperature occurred somewhat distant from the wall only when soffit height was 0.1 m but occurred very close to the wall in the other soffit heights. In the other opening sizes, the maximum temperature occurred more distant from the wall as soffit height was raised. Accordingly, the area of the soffit hit by the jet plume can roughly be inferred from the curves in Figure 4.

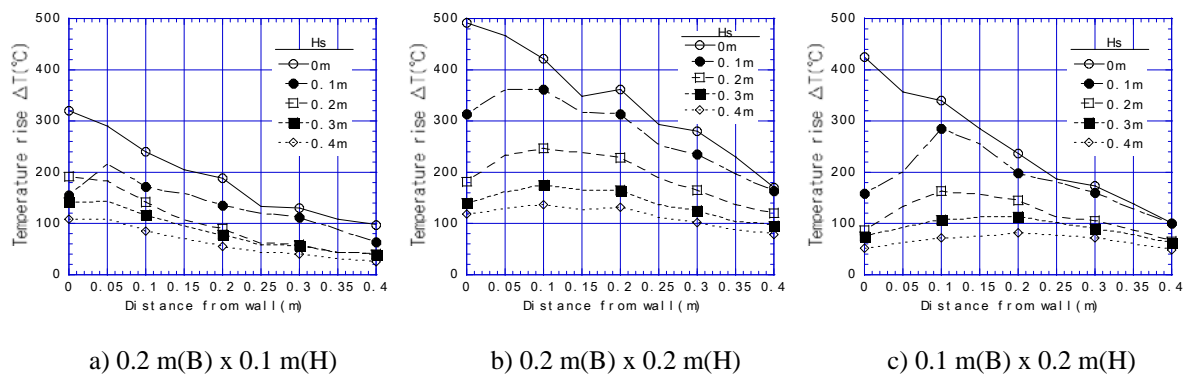


**Figure 4:** Temperature distribution beneath the soffit (0.4 m long) placed at different heights in the small-size model.

#### Temperature distribution at the far end of the soffit

Figure 5 shows, for each opening size, temperature distribution along the far end of the soffit (between

the center and one corner of the soffit) at a soffit height of 0.2 m. The curves correspond to different soffit lengths. Temperature at the center of the far end of the soffit increased as soffit length was reduced as long as the soffit was hit by the plume axis. As soffit length was increased, the maximum temperature along the far end of the soffit and the decline of temperature from the center to the corner decreased.

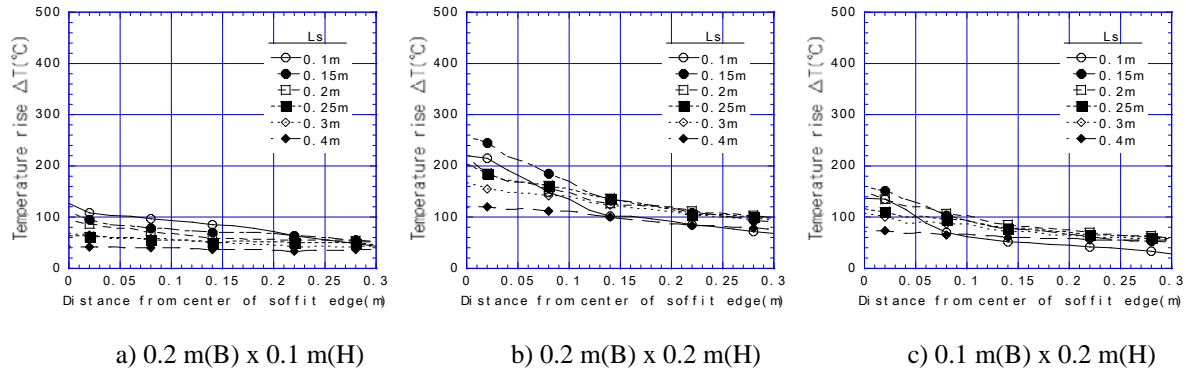


**Figure 5:** Temperature distribution along the far end of the soffit at a soffit height of 0.2 m.

### Confirmation of similarity

The similarity of plume temperature distributions was investigated in the small- and medium-size models having geometrically similar opening and soffit dimensions. Non-dimensional temperature  $\Theta(\zeta, \eta)$  was used to evaluate the similarity of plume temperature distributions. Here, the nondimensional location  $(\zeta, \eta)$  of a jet plume is given by:

$$\zeta = l/B \quad (1)$$

$$\eta = h/B \quad (2)$$

where “l” indicates horizontal distance from the wall and “h” indicates vertical distance from the upper edge of opening. According to Yokoi, non-dimensional temperature is given by<sup>5,7</sup>:

$$\Theta_{(\zeta, \eta)} = \frac{\Delta T_{(\zeta, \eta)} r_0^{5/3}}{\sqrt[3]{T_\infty Q^2 / c_p^2 \rho^2 g}} \quad (3)$$

where  $r_0$  is calculated from:

$$r_0 = \sqrt{\frac{BH}{2\pi}} \quad (4)$$

As relationship between density and temperature of opening jet plume can be expressed as

$$\rho T = \rho_\infty T_\infty \quad (5)$$

Equation 3 can be rewritten:

$$\Theta_{(\xi,\eta)} = \frac{\frac{\Delta T_{(\xi,\eta)}}{T_\infty}}{Q_{r0}^{*2/3} \left( \frac{T}{T_\infty} \right)^{2/3}} \quad (6)$$

where  $Q_{r0}^*$  is the non-dimensional heat release rate of the jet plume expressed as:

$$Q_{r0}^* = \frac{Q}{\rho_\infty c_p T_\infty g^{1/2} r_0^{5/2}} \quad (7)$$

As the rate of outflow of air via an opening from compartment can be approximated by <sup>8</sup>:

$$R_{fo} \approx (0.5 \sim 0.52)BH^{3/2} \quad (8)$$

the heat release rate  $Q$  of the plume are calculated from <sup>9</sup>:

$$Q = c_p R_{fo} (T_f - T_\infty) \quad (9)$$

$$= (0.5 \sim 0.52)c_p BH^{3/2}(T_f - T_\infty) \quad (10)$$

In Figure 6, the small-scale model had an opening width of 0.2 m, an opening height of 0.2 m, a soffit length of 0.1 m, and a soffit height of 0.2 m. The medium-size model had an opening width of 0.6 m, an opening height of 0.6 m, a soffit length of 0.3 m, and a soffit height of 0.6 m. The non-dimensional temperature distribution of a jet plume affected by the soffit in each model shows a good similarity between the two distributions.

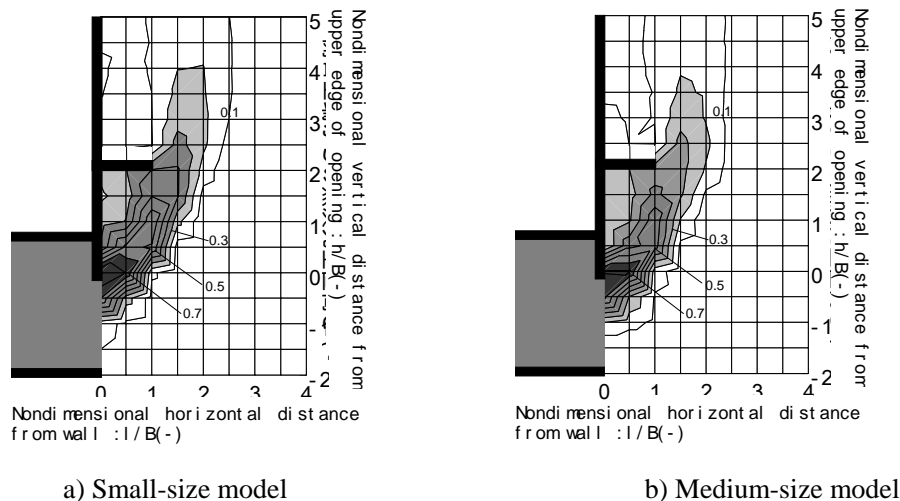


**Figure 6:** Non-dimensional temperature distribution of a jet plume.

(Interval of non-dimensional temp = 0.1).

Under the same conditions as those of Figure 6, the non-dimensional temperature distribution beneath the soffit and the non-dimensional temperature distribution along the far end of the soffit in each



model are shown in Figures 7 and 8, respectively. The horizontal axis in Figure 7 represents non-dimensional distance  $\zeta$  from the wall, while the curves correspond to different non-dimensional soffit heights. The figure indicates that the position of maximum temperature (i.e. area of the soffit hit by the plume) is almost the same if non-dimensional soffit height  $\eta$  is the same. The horizontal axis in Figure 8 represents non-dimensional horizontal distance  $Y_s/B$  (where  $Y_s$  is distance from the center of the far end of the soffit), while the curves correspond to different non-dimensional soffit heights. The figure indicates that non-dimensional temperature distributions are nearly the same between the small- and medium-size models and that non-dimensional temperature distributions along the far end of the soffit for different non-dimensional soffit lengths can broadly be approximated to Gaussian distributions.

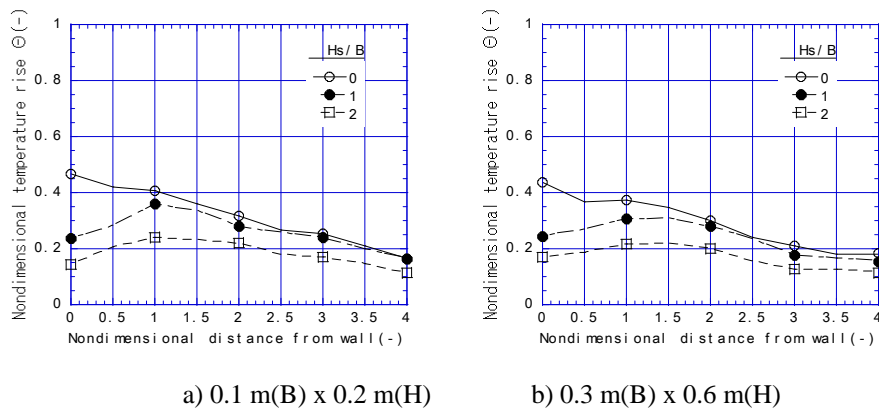


**Figure 7:** Nondimensional temperature distribution of beneath the soffit in each model.

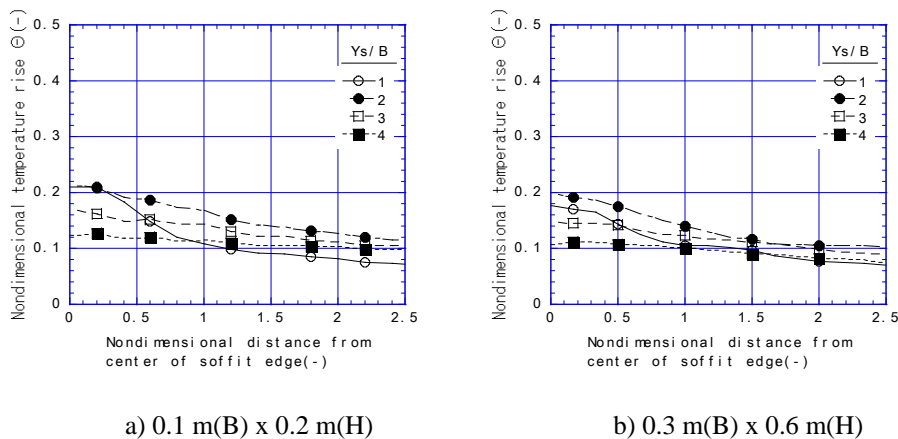


**Figure 8:** Nondimensional temperature distribution along the edge of the soffit in each model

### Estimation of jet plume temperatures

Figure 9 shows distributions of plume axis temperatures for different soffit heights in the case of an opening width of 0.2 m and an opening height of 0.2 m<sup>[10]</sup>. The horizontal axis represents non-

dimensional temperature  $\Theta$  calculated by using Equation 3 from measured plume axis temperatures. The vertical axis represents non-dimensional length  $z/r_0$ , where  $z$  is length measured along the plume axis and  $r_0$  is equivalent opening radius. The solid curves in Figure 9 represent distributions of non-dimensional plume axis temperatures without the presence of a soffit.

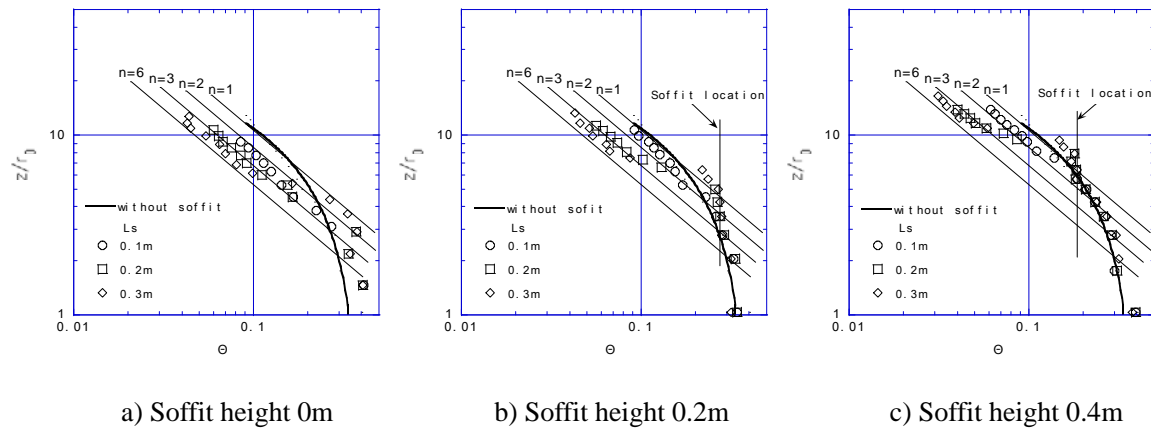


**Figure 9:** Distributions of plume axis temperatures for different soffit heights in the case of a opening width of 0.2 m and a opening height of 0.2 m.

The following remarks are made with reference to Figure 9.

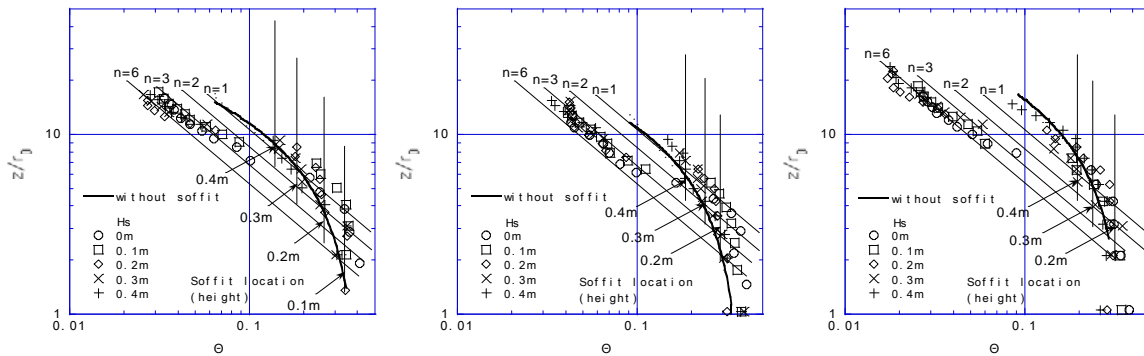
Before the jet plume hits the soffit, the distribution of plume temperatures is not significantly altered by the presence of the soffit regardless of its height. This does not apply to the soffit height of 0 m because the plume ejected from the opening immediately hits the soffit.

After hitting the soffit, the jet plume moves laterally to the far end of the soffit. The plume shows little temperature decrease immediately after hitting the soffit in spite of an increase in non-dimensional length  $z/r_0$ . Then, plume temperature gradually decreases.

After passing the far end of the soffit, the jet plume's temperature decreases steeply and then approaches a constant rate of temperature decrease. The constant rate is reached at lower temperatures as soffit length is increased. Yokoi suggested that the temperature distribution of the jet plume after passing the far end of the soffit would become close to that of the plume not blocked by a soffit above the opening. The results of the present study indicate that temperature distribution for a soffit length of 0.1 m becomes close to the distribution corresponding to a opening aspect ratio of  $n=2$ , as suggested by Yokoi. However, temperature distribution for a soffit length greater than 0.1 m becomes close to the distribution corresponding to a opening aspect ratio greater than 2.

Figure 10 shows distributions of plume axis temperatures when soffit length is 0.3 m for different opening sizes and soffit heights. As is the case with Figure 9, the horizontal and vertical axes represent non-dimensional temperature  $\Theta$  and non-dimensional length  $z/r_0$ , respectively.

Figure 10 indicates that the non-dimensional temperature distribution of the jet plume after passing the far end of the soffit does not vary significantly with soffit height if soffit length is unchanged. The temperature distribution of the jet plume after passing the far end of the soffit becomes closer to the temperature distribution without a soffit as the opening aspect ratio is reduced.



a) 0.1 m(width:B) x 0.2 m(height:H) b) 0.2 m(width:B) x 0.2 m(height:H) c) 0.2 m(width:B) x 0.1 m(height:H)

**Figure 10:** Distributions of plume axis temperatures when soffit length is 0.3 m for different opening sizes and soffit heights.

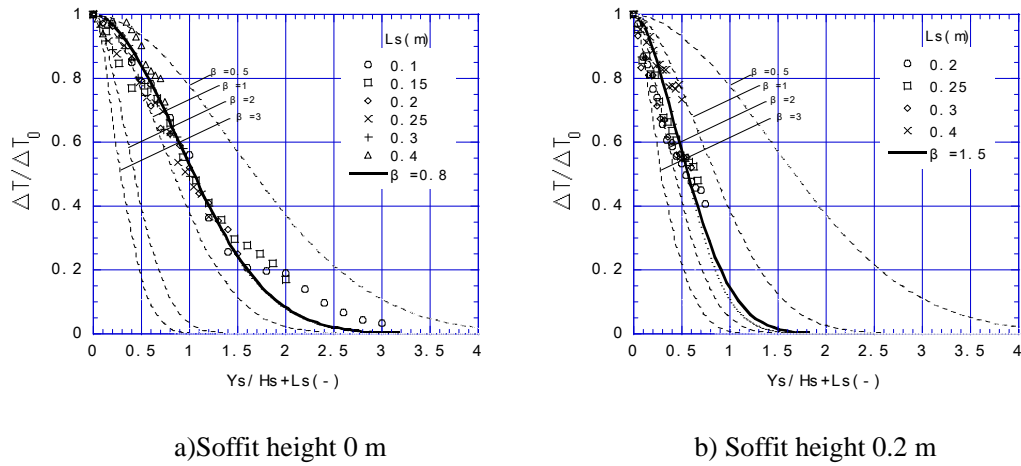
#### Horizontal temperature distribution along the far end of the soffit

Figure 8 indicates that the temperature distribution along the far end of the soffit can broadly be approximated to a Gaussian distribution with the plume axis being the center of the distribution. It has been argued previously that the distribution of fire plume temperatures in a free space can be approximated to a Gaussian distribution as described by the following equation<sup>11 to 13</sup>:

$$\frac{T}{T_0} \left( = \frac{T - T}{T_0 - T} \right) = e^{-\kappa^2 \beta^2} \quad (11)$$

In an attempt to apply Equation 11 to the plume temperature distribution along the far end of the soffit,  $\kappa$  was deduced by dividing the distance from the plume axis along the far end of the soffit ( $Y_s$ ) by the sum of soffit height and soffit length ( $H_s + L_s$ ). The value of  $\beta$ , the half-width ratio of Gaussian temperature distribution, was obtained from experimental results.

Figures 11 and 12 show non-dimensional horizontal temperature distributions along the far end of the soffit placed at different heights in small- and intermediate-size models. The experimental results shown in the figures are in good agreement with the Gaussian distributions calculated from Equation 11. The values of  $\beta$  in the equation are in the range of 0.5 to 2 under the experimental conditions studied<sup>14,15</sup>. A comparison of Figures 11 and 12 indicates that  $\beta$ -values are nearly the same if experimental conditions are geometrically similar.



**Figure 11:** Nondimensional horizontal temperature distributions along the far end of the soffit placed at different heights in small-size models.

Opening size 0.1 m (width:  $B$ ) x 0.2 m (height:  $H$ ).

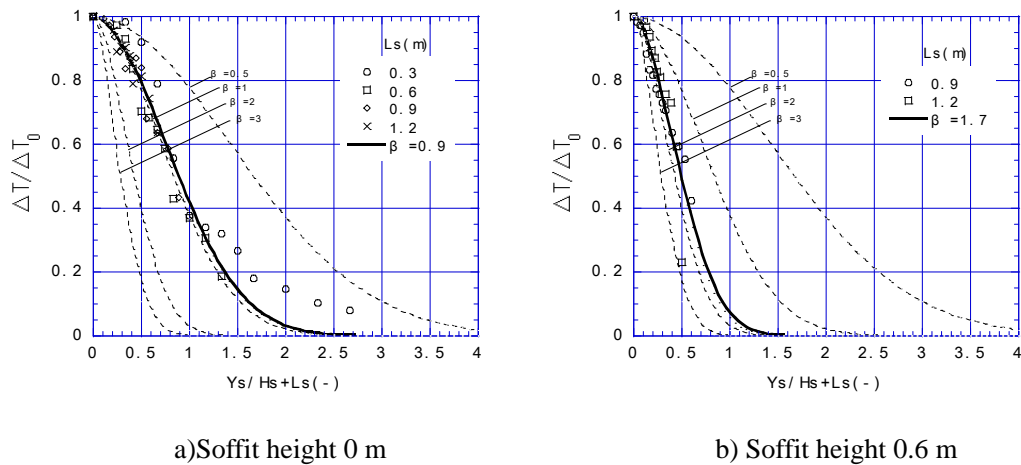


**Figure 12:** Nondimensional horizontal temperature distributions along the far end of the soffit placed at different heights in medium-size models. Opening size 0.3 m (width:  $B$ ) x 0.6 m (height:  $H$ ).

Figure 13 shows a good correlation between  $\beta$  and the sum of soffit height  $H_s$  and soffit length  $L_s$  divided by opening width  $B$ .

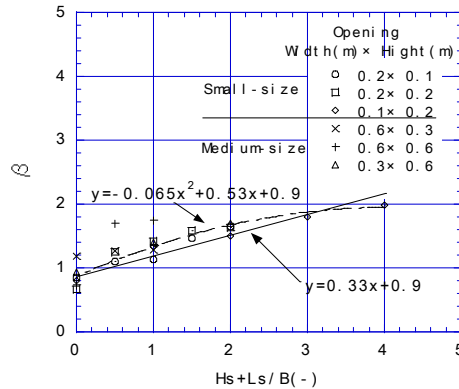


Figure 13: Correlation between  $\beta$  and  $(Hs+Ls)/B$ .

## CONCLUSIONS

- The vertical distribution of jet plume temperatures at an opening does not depend significantly on the presence of a soffit as long as the opening size is unchanged.
- The location of the jet plume axis between the opening and the soffit does not depend significantly on the presence of the soffit.
- If the soffit is long enough to be hit by the plume axis, temperature at the center of the far end of the soffit and the decline of temperature from the center to the corner increase as soffit length is reduced.
- The non-dimensional temperature distributions of jet plumes in geometrically similar small- and medium-size models having a soffit, are nearly identical for each non-dimensional soffit length (i.e. the same area of the soffit is hit by the plume).
- The distribution of jet plume temperatures along the far end of the soffit can be approximated to a Gaussian distribution with the plume axis being the center of the distribution and  $\beta$  -values in the range of 0.5 to 2. There is a good correlation between  $\beta$  and the sum of soffit height  $H_s$  and soffit length  $L_s$  divided by opening width  $B$ .

## ACKNOWLEDGMENTS

The authors wish to thank Mr. Yuji HORI (Yasuda Fire and Marine Insurance Co. LTD., formerly graduate student of Tokyo University of Science) for supporting the experiments.

## **NOMENCLATURE**

B	Opening width (m)
$C_p$	Specific heat of air (kJ/kgK)
g	Gravitational acceleration ( $m/s^2$ )
H	Opening height (m)
$H_s$	Soffit height (m)
$L_s$	Soffit length (m)
Q	Heat release rate of external flame (kW)
$R_{fo}$	Rate of air outflow (kg/s)
$r_0$	Equivalent opening radius (m)
T	External flame temperature (K)
$T_f$	Temperature in fire compartment (K)
$T_\infty$	Ambient temperature (K)
$\Delta T$	Temperature rise (K)
$Y_s$	Distance from the plume axis along the far end of the soffit
$Z_n$	Height of neutral plane(m)
z	Distance along Plume axis from opening(m)
$\Theta$	Non-dimensional temperature (-)
$\alpha$	Opening flow coefficient (-)
$\beta$	half Width (-)
$\rho$	Air density( $kg/m^3$ )
$\rho_f$	Air density of air in fire compartment ( $kg/m^3$ )
$\rho_\infty$	Ambient air density ( $kg/m^3$ )

## REFERENCES

1. S. Yokoi: A Study on Fire Spread caused by Opening Jet Plume, Japanese Ministry of Construction, Building Research Institute Report 34, 1960.
2. American Iron and Steel Institute: Fire Safe Structural Steel – A Design Guide , 1979.
3. R. Jansson, B. Onnermark: Flame Heights Outside Openings, FOA Report, C 20445-A3,1982.5.
4. Japanese Ministry of Construction: Total Fire Safety Design System of Buildings, Vol2, The Building Center of Japan, 1989(in Japanese).
5. J. Yamaguchi, Y. Iwai, T. Tanaka, K. Harada, Y. Ohmiya, T. Wakamatsu: Applicability of Nondimensional Temperatures of Window Jet Plume, Journal of Architecture, Planning and Environmental Engineering (Transactions of Architectural Institute of Japan), pp.1-7, No513, 1998.11(in Japanese).
6. L.Y. Cooper, M. Harkeroad, J. Quintiere, W. Rinkinen: An Experimental Study of Upper Hot Layer Stratification in Full-Scale Multiroom Fire Scenarios, Journal of Heat Transfer, Vol.104, pp.741-749, 1982.11.
7. S. Yokoi: On the Heights of Flames from Building Cribs, Bull. of the Fire Prevention Society of Japan, Vol.7, No.2, pp41-45, 1958.3(in Japanese).
8. D. Drysdale: An Introduction to Fire Dynamics, Second Edition, John Wiley & Sons, pp 330-331, 2000.4.
9. T. Tanaka: Introduction of Fire Safety Engineering, The Building Center of Japan, 1993(in Japanese).
10. S. Yokoi: Trajectory of Hot Gas spurting from a window of a burning Concrete House, Bull. of The Fire Prevention Society of Japan, Vol.8, No.1, pp1-5,1958.6(in Japanese).
11. E. E. Zukoski, T. Kubota, B. Cetegen: Entrainment in Fire Plume, Fire Safety Journal, Vol.3, pp 107-121, 1980/1981.
12. S. Yokoi: Upward Current from Heat Source - Vertical Distribution of Velocity and Temperature-, Bull. of The Fire Prevention Society of Japan, Vol.3, No.1, 1953 (in Japanese).
13. S. Yokoi: Upward Current from Heat Source - Horizontal Distribution of Velocity and Temperature-, Bull. of The Fire Prevention Society of Japan, Vol.4, No.1, 1954.in Japanese).
14. O. Sugawa, T. Hosozawa, N. Nakamura, A. Itoh, Y. Matsubara: Flow Behaviour under Sloped Ceiling, 15th MEETING OF THE UJNR PANEL ON FIRE RESEARCH AND SAFETY, Vol.2, 2000.3.
15. D. Momita: Flow Behavior of an Ejected Fire Flame/Plume from an Opening Effectuated by External Side Wind, a master's thesis of the Science University of Tokyo, 1997(in Japanese).